Coordination of Some Simple Molecules onto $W(CO)_5$ in the Gas Phase

Motohiro JYO-O, Hideki TAKEDA, Kenji OMIYA, Yo-ichi ISHIKAWA,* and Shigeyoshi ARAI
Material Science and Technology, Kyoto Institute of Technology, Matsugasaki, Sakyo-ku, Kyoto 606
(Received June 17, 1993)

In the gas phase at room temperature, the coordination process of NH_3, C_2H_4, CF_4, SF_6, and Xe onto "naked" $W(CO)_5$, selectively prepared by pulsed 355-nm laser photolysis of $W(CO)_6$, was investigated by laser-based time-resolved infrared absorption spectroscopy. $W(CO)_5$ reacted with these reactant gases, except for CF_4 and SF_6, to make a simple coordination complex, $W(CO)_5(L)$, where L is NH_3, C_2H_4, or Xe. The bimolecular rate constants for these reactions were $(5.6\pm0.6)\times10^6$ $Torr^{-1}$ s^{-1} for $W(CO)_5+NH_3$, $(2.8\pm0.5)\times10^6$ $Torr^{-1}$ s^{-1} for $W(CO)_5+C_2H_4$, and $(1.0\pm0.3)\times10^5$ $Torr^{-1}$ s^{-1} for $W(CO)_5+Xe$. $W(CO)_5Xe$ was unstable owing to its weak interaction with the coordinatively unsaturated tungsten center, the unimolecular decomposition rate of which was about 1.0×10^5 s^{-1}, but $W(CO)_5(NH_3)$ and $W(CO)_5(\eta^2\text{-}C_2H_4)$ were stable under our experimental conditions. The band shifts of C–O stretching modes observed in the coordination of NH_3 as a typical σ-donor, C_2H_4 as a typical π-acceptor, and Xe as a weak σ-donor could interpreted by MO considerations.

Since the first experimental evidence for the existence of group VI transition metal pentacarbonyls was reported in 1962 by Stoltz et al.,[1] there have been a number of spectroscopic studies of coordinatively unsaturated transition metal pentacarbonyls such as $Cr(CO)_5$, $Mo(CO)_5$, and $W(CO)_5$.[2] Such compounds are likely to be reactive because this "coordinatively unsaturated" species with 16 valence electrons at the metal center is 2 electrons short of the stable 18-electron configuration. That the visible and infrared absorption bands of the pentacarbonyls are extremely sensitive to the surrounding species, matrix or solvent molecules,[3] reflects such reactivity. The shifts have been interpreted in terms of "stereospecific" effects due to interaction of the pentacarbonyl with a surrounding molecule in its vacant site with the retention of the C_{4v} configuration, although the effects on the infrared are commonly obscured by what is called the "solvent" effect, similar to the effects observed for a coordinatively saturated metal carbonyl, $M(CO)_6$.[3] Pico- and femto-second transient absorption spectroscopy of $M(CO)_6$ photolysis is now making clear the production ($\leq$500 fs)[4] and complexation (~a few picoseconds)[4,5] features of "naked" $M(CO)_5$ and the relaxation processes of the product complex, $M(CO)_5L$, in liquid phase at room temperature.

The C–O stretching frequencies of transition metal carbonyl compounds are very sensitive to the oxidation state of the metal center.[6] As the oxidation state varies with the number of coordinatively unsaturated sites or with the coordination species, the observation of C–O stretching frequencies may provide information about interactions between the unsaturated transition metal center and coordination molecules, that is, the metal's d-orbitals and the ligand's molecular orbitals. Studies of pulsed UV laser photolysis of transition metal carbonyls in the gas phase have analyzed their primary photophysical and photochemical processes and also provided a convenient means for selective production of naked coordinatively unsaturated sites, which are free from the solvent effect.[7] If an appropriate reactant molecule, even an unlikely ligand such as alkanes,[8] N_2O, CF_2Cl_2,[9] or rare gases,[10] is added to the gaseous photolysis system of a metal hexacarbonyl, the coordination process of the molecule onto the photoproduced naked coordinatively unsaturated site(s) can be directly pursued by conventional sub-microsecond time-resolved infrared (TRIR) absorption spectroscopy. The TRIR absorption measurement of direct coordination processes of some simple molecules onto naked coordinatively unsaturated metal sites in the gas phase makes possible discussion about the interaction between d-orbitals at transition metal centers and ligand orbitals on the base of C–O stretching shifts.

Amine and olefin are typical σ-donor and π-acceptor ligands and reports of spectroscopic research on $W(CO)_5$(amine) or $W(CO)_5$(olefin) in the condensed phase have been published.[11,12] However, no gas-phase infrared absorption spectrum of $W(CO)_5(NH_3)$ or $W(CO)_5(C_2H_4)$ as the simplest complex has been reported, probably owing to thermal instability. In a recent letter, we reported preliminary infrared absorption spectra of these two complexes in the gas phase, which are free from solvent effects.[13] In this paper, we report the reactivity of naked $W(CO)_5$ with some simple molecules (C_2H_4, NH_3, CF_4, SF_6, Xe) together with details of our experimental setup and discussion about the direct coordination processes at room temperature.

Experimental

The apparatus for laser-based TRIR absorption spectroscopy mainly consists of two lasers, one a pulsed UV laser as a photolysis light source and the other a cw IR laser as a probe light source; the apparatus (Fig. 1) resembles an existing TRIR absorption spectroscopy apparatus.[14—17] The probe source was a home-made liquid-N_2-cooled cw-CO laser, the spectral range of which was 1650-2050 cm^{-1} with the spectral resolution of about 4 cm^{-1}.[18] The resonance cavity is formed by an original ruling grating blazed at 5.4 μm (Optometric Co., model ML-401) and a 90% partial reflection-antireflection coating, with a 3-m radius of ZnSe plano concave mirror (Lasermate Co.) for output coupling.

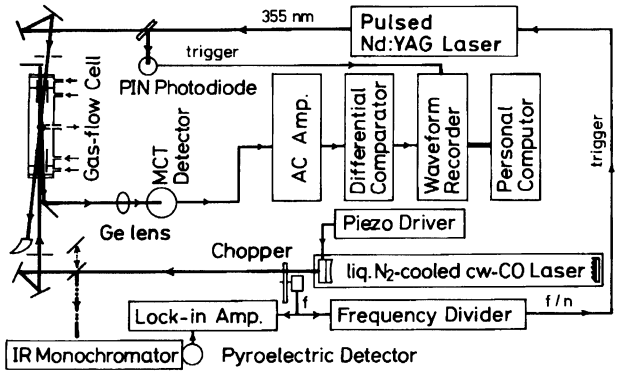

Fig. 1. Schematic diagram of apparatus for time-resolved infrared (TRIR) absorption spectroscopy.

The resonance length was finely adjusted by a piezoelectric translator (Lansing Co., model 21-934: maximum expansion, 12 μm) holding the output mirror, in order to obtain a single lasing line of CO transition. The discharge in a 1.4-m-long Pyrex tube (30 mm in diameter) is split into two parts, with a common cathode in the middle. The gases are mixed, passed into the discharge area through the anode ports, and pumped out through the cathode port. The region between the two anodes is about 1.15 m wide, which roughly coincides with the cold active region. The discharge tube has two Brewster angle CaF_2 ($60\times40\times5^t$) windows on both sides. A typical gas mixture consisted of 4.0 Torr He, 0.3 Torr N_2, and a small amount ($\leq$0.05 Torr) of CO (1 Torr=133.322 Pa), which were varied suitably to achieve optimum lasing for an individual CO transition. A total of about 100 lasing transitions can be obtained between a few milliwatts and 300 mW at a discharge power input of about 20 W (ca. 3.5 kV×6 mA). The pressure was measured at the exhaust pipe with an absolute pressure gauge (MKS Baratron, model 122AA-10 Torr). The accuracy of the CO laser wavenumber, monitored with a calibrated monochromator (Ritsu Ouyou-Kougaku Co., MC-20L) equipped with a 5-μm blaze grating with 122 grooves per millimeter, and a pyroelectric sensor (Hamamatsu, P3782), was estimated to be less than ±4 cm^{-1}. A pulsed Nd:YAG laser (Spectron SL803, λ=355 nm) was used as the UV photolysis source. The typical fluence was about 10 mJ cm^{-2}. The probe IR laser light twice passed the 15-cm reaction cell, almost collinear with the photolysis beam. Care was taken to ensure full overlap of the probe beam ($\leq$2 mm in diameter) with the UV-irradiated portion of the sample volume (ca. 8 mm in diameter).[17b] Transient species are monitored through their absorption of the probe laser beam as detected by a combination of a New England Research Center MCT detector (model MPC11-2-A1) and a preamplifier (model PA-S6: bandwidth, 20—3 MHz). The preamplified signal is amplified further in a Tektronix differential comparator (model 7A13) and recorded by a Biomation 8100 transient digitizer. The UV laser-light signal picked up with a PIN photodiode sensor (Hamamatsu, model S1722-02) was used as a trigger signal for the transient digitizer. The cw probe beam is chopped by a mechanical chopper (Scitec Ins.) at ca. 500 Hz, and the photolysis laser is synchronized with the chopped beam at 10 Hz by a frequency divider. This arrangement allows the recording of small signal changes at high sensitivity and simultaneous measurement of the total signal strength. The latter is required when a TRIR absorption spectrum is constructed from a series of kinetic runs without the necessity of extra monitoring of probe laser power from run to run or from line to line. Biomation records are transferred, shot by shot, to a personal computer (NEC PC-9801 RX) where they are averaged and stored. In this study, a typical average shot was 50 for each kinetic trace. The TRIR difference absorption spectra are extracted from a series of kinetic absorption measurements at different probe wavelengths. The overall rise-time of the system was ca. 800 ns.

$W(CO)_6$ (Aldrich, 99%) was degassed by several freeze-pump-thaw cycles with liq. N_2 and used without further purification. Ammonia (Nihon Sanso Co., $\geq$99.999%), Ethylene (Takachiho Co., $\geq$99.9%), CF_4 (Takachiho, $\geq$99.999%), SF_6 (Takachiho, $\geq$99.99%), and Xe (Iwatani Co., $\geq$99.995%) were used without further purification except for degassing several times. Ar (Air Products, research grade) was used as supplied. $W(CO)_6$, either neat or mixed with reactant gas, was allowed to flow slowly through the brass reaction cell with two CaF_2 windows that had an effective path length of 15 cm for UV photolysis light and of 30 cm (15 cm×2) for IR probe light. Pressures were measured with an absolute pressure gauge (MKS Baratron, model 220BH-10 Torr) attached to the cell. Additional Ar gas flow in the vicinity of the windows was used to help prevent metal deposition on the windows.

Results

Reactivity of $W(CO)_5$ with Typical Ligands (NH_3 and C_2H_4). Photolysis at 355 nm of gas-phase $W(CO)_6$ produces the monounsaturated species $W(CO)_5$ exclusively at the $^1A_1$ ground state at moderate fluences.[9] Figure 2 shows time-resolved difference absorption spectra observed after the 355-nm photol-

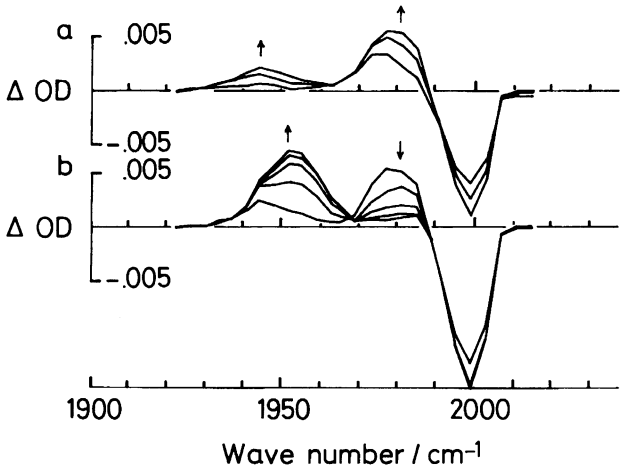

Fig. 2. Time-resolved difference absorption spectra following 355-nm laser photolysis of $W(CO)_6$ (ca. 10 mTorr) in the presence of NH_3 (0.05 Torr) at a total pressure of 6.0 Torr with balance Ar: (a) early spectra taken at 0.2-μs intervals over 0.4—0.8 μs; (b) later spectra taken at 1-μs intervals over 1-5 μs. An arrow points upward indicates an increase of ΔOD and an arrow points downward indicates a decrease.

ysis of $W(CO)_6$ (ca.10 mTorr; 1 Torr=133.322 Pa) in the presence of NH_3 (0.05 Torr) at a total pressure of 6.0 Torr with Ar for balance. The TRIR spectra observed within 0.8 μs after the photolysis pulse (Fig. 2a) show the photoproduction of "hot" $W(CO)_5$ with broad bands at about 1980 and 1943 cm^{-1} together with the decomposition of $W(CO)_6$, corresponding to a ΔOD decrease at about 1999 cm^{-1}. In absence of NH_3, these two bands should show the previously observed sharpening and shifting to the blue associated with relaxation of internal energy to produce a spectrum similar to that of fully relaxed $W(CO)_5$[19]. The 1943-cm^{-1} band has been identified as the low-frequency band of the A_1 mode and the 1980-cm^{-1} band has been identified as the E mode of C_{4v} symmetry.[3,19–21] As Ar, used as the balance gas, does not coordinate on $W(CO)_5$ at room temperature,[10] the species with these two absorption bands can be considered to be naked $W(CO)_5$. Later (Fig. 2b, >1μs), a new absorption band centered at 1952 cm^{-1}, with a shoulder at about 1943 cm^{-1} (not clear because of overlap with the intense absorption band), has grown as the $W(CO)_5$ band(s) decreases. The isosbestic point is at ca. 1968 cm^{-1}. The reaction is complete after ca. 6—7 μs, and the transient absorption does not change during observation (20 μs).

Figure 3 shows typical time dependence of absorption features at 1981 cm^{-1} (curve I) and 1952 cm^{-1} (curve II) in the presence of NH_3 (0.10 Torr) (b) together with those in the absence of NH_3 (a). At the former wave number, absorption is mainly due to $W(CO)_5$ and at the latter, absorption is mainly due to the NH_3-induced transient. Without NH_3, the absorption at 1981 cm^{-1} is established near to the rise time of our experimental system and then decays slowly. The $W(CO)_5$ decay process has been assigned to the following binucleation reaction.[19] At 1952 cm^{-1}, secondary absorption is attributed to $W_2(CO)_{11}$ produced through reaction 1.

$$W(CO)_5 + W(CO)_6 \rightarrow W_2(CO)_{11} \quad (1)$$

In the presence of NH_3, the 1981-cm^{-1} absorption decays more rapidly while the absorption at 1952 cm^{-1} grows in with matching kinetics. Both rates also depend linearly on the NH_3 pressure with a similar slope. These experimental results suggest that the new complex can be assigned to a simple coordination compound $W(CO)_5(NH_3)$ formed through reaction 2, the gas-phase IR absorption spectrum of which is shown in

$$W(CO)_5 + NH_3 \rightarrow W(CO)_5(NH_3) \quad (2)$$

Fig. 4a together with a $W(CO)_5(\eta^2\text{-}C_2H_4)$ spectrum (Fig. 4b) mentioned below and a naked $W(CO)_5$ spectrum (Fig. 4c) for reference.

A similar coordination reaction was observed after the photolysis of $W(CO)_6$ in the presence of C_2H_4

$$W(CO)_5 + C_2H_4 \rightarrow W(CO)_5(\eta^2 - C_2H_4) \quad (3)$$

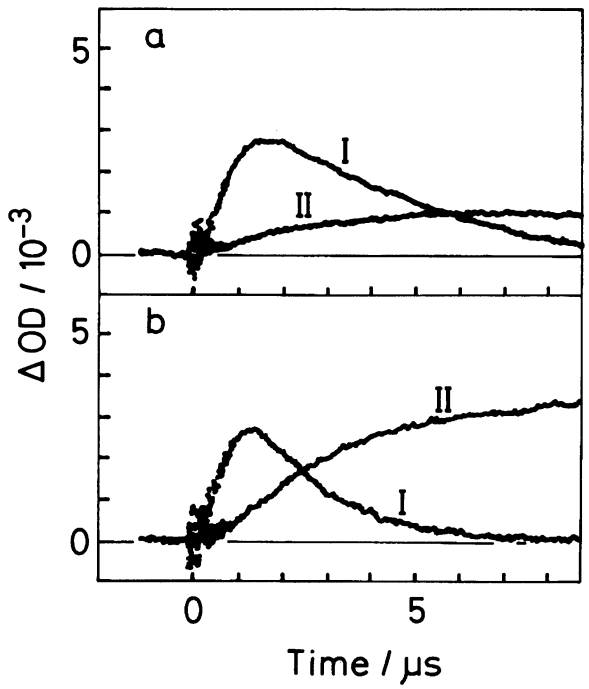

Fig. 3. Typical transient absorption observed in the 355-nm laser photolysis of $W(CO)_6$ (ca. 10 mTorr) (a) without NH_3 and (b) with NH_3 (0.10 Torr) at a total pressure of 6.0 Torr with balance Ar. (I) $W(CO)_5$ monitored at 1981 cm^{-1}; (II) $W(CO)_5NH_3$ monitored at 1952 cm^{-1}.

(reaction 3). The IR absorption spectrum observed 1.5 μs after photolysis in the presence of C_2H_4 (ca. 0.2 Torr) is shown in Fig. 4b, which has two absorption bands at 1968 cm^{-1} and about 1985 cm^{-1}. The transient spectrum development in the early-time region (≤1 μs) was similar to the spectrum observed in the absence of reactant, when the hot $W(CO)_5$ is relaxed. In the later-time region (>1 μs), the bands attributable to naked $W(CO)_5$ gradually disappear and synchronously, new absorption bands grow at about 1985 and 1968 cm^{-1}. Kinetic analysis also gives evidence for assignment of these two absorption bands to $W(CO)_5$ (η^2-C_2H_4). From comparison with the IR absorption frequencies of $W(CO)_5(\eta^2\text{-}C_2H_4)$ in hexane solution at room temperature (1953 (E) and 1973 cm^{-1} (A_1)),[2a] the bands centered at 1985 and 1968 cm^{-1} can be assigned to a low frequency of the A_1 mode and an E mode of C–O stretching, respectively.

Figure 5 shows the ligand pressure dependence of the decay rate of $W(CO)_5$ and of the production rate of $W(CO)_5L$ (L=NH_3 and C_2H_4). The decay of $W(CO)_5$ was monitored at 1981 cm^{-1}, the production of $W(CO)_5(NH_3)$ was monitored at 1952 cm^{-1}, and the production of $W(CO)_5(\eta^2\text{-}C_2H_4)$ was monitored at 1968 cm^{-1}. Total pressure with balance Ar and the $W(CO)_6$ pressure were kept constant at about 10 Torr and 10 mTorr, respectively. The single-straight line behavior of these processes is consistent with the stoichiometry

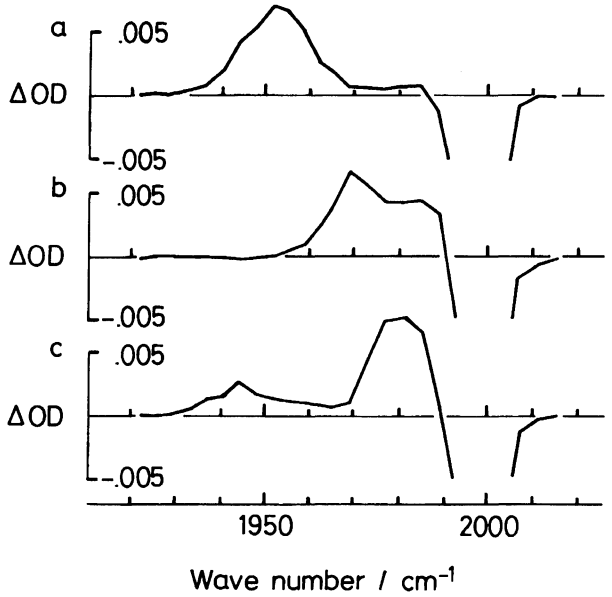

Fig. 4. Infrared absorption spectra of the complexes $W(CO)_5L$ (L=NH_3 and C_2H_4) observed after gas-phase 355-nm photolysis of mixtures of $W(CO)_6$ (ca. 10 mTorr) and L at a total pressure of 6.0 Torr with balance Ar. The following pressures of L were present in the photolysis mixtures: (a) NH_3, 0.05 Torr; (b) C_2H_4, 0.2 Torr. The spectra were recorded (a) 5.0 μs and (b) 1.5 μs after photolysis. The spectrum in (c) illustrates the absorption due to fully relaxed $W(CO)_5$ at room temperature.

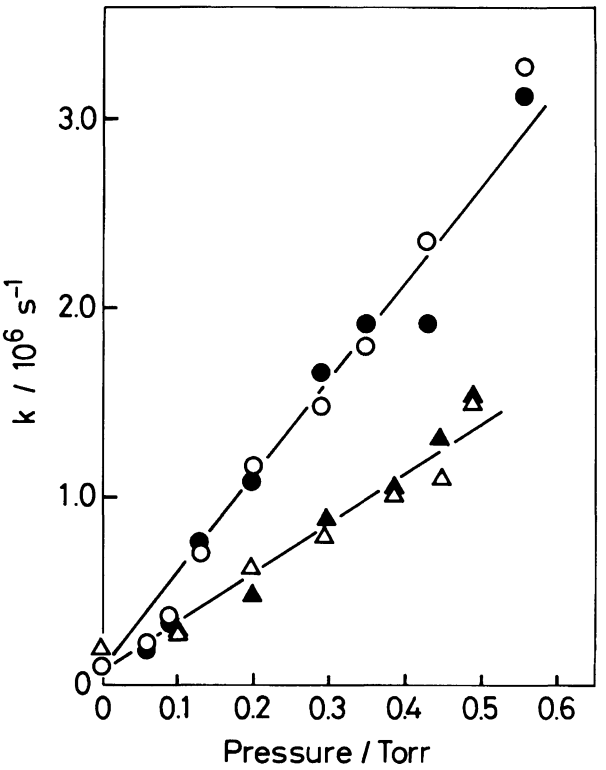

Fig. 5. Reactant pressure dependence of the decay rate (k'_d) of $W(CO)_5$ and the production rate (k'_p) of $W(CO)_5L$ after 355-nm laser photolysis of mixtures of $W(CO)_6$, Ar, and reactant. $W(CO)_6$ and total pressure were kept constant at about 10 mTorr and 10 Torr with balance Ar. The decay rates were monitored at 1981 cm^{-1} for NH_3 (○) and for C_2H_4 (△) additions. The production rates were monitored at 1950 cm^{-1} for NH_3 (●) and at 1969 cm^{-1} for C_2H_4 (▲) additions.

of the coordination reactions 2 and 3. The slopes give bimolecular rate constants of $(5.6\pm0.6)\times10^6$ $Torr^{-1}$ s^{-1} for NH_3 coordination and $(2.8\pm0.5)\times10^6$ $Torr^{-1}$ s^{-1} for C_2H_4 coordination. The y-intercept of the lines, ca. 2×10^5 s^{-1}, is attributed to the binuclear reaction of $W(CO)_5$ with the parent hexacarbonyl (reaction 1). In general, there are back-reactions corresponding to reactions 1, 2, and 3, respectively. However, the contribution of these back-reaction seems to be negligible at this temperature because of the large stabilization energy of the product. The large internal degrees of freedom of the product, $W_2(CO)_{11}$, $W(CO)_5(NH_3)$, or $W(CO)_5(C_2H_4)$, also suggest the consideration that the rate constant obtained at a total pressure of 10 Torr with Ar buffer gas is the bimolecular rate constant at the high-pressure limit.

Reactivity of $W(CO)_5$ with Unlikely Ligands (CF_4, SF_6, and Xe). The TRIR spectra following 355-nm laser photolysis of $W(CO)_6$ in the presence of CF_4 (5.0 Torr) or SF_6 (5.0 Torr) at the total pressure of 10 Torr with balance Ar did not show any difference from TRIR spectra observed in the 355-nm photolysis of pure $W(CO)_6$ with balance Ar, except in the relaxation process of hot $W(CO)_5$. This finding suggests that the interaction of $W(CO)_5$ with CF_4 or SF_6 is weak in forming coordination compounds under our experimental conditions.

Figure 6 shows the TRIR spectra observed after 355-nm laser photolysis of $W(CO)_6$ (ca. 10 mTorr) in the presence of Xe (ca. 6.0 Torr) at a total pressure of 10 Torr with balance Ar, taken at 0.4 μs intervals over a 0.4- to 2.0-μs range. The TRIR spectra observed immediately after photolysis (≤1.0 μs) show the photoproduction of hot $W(CO)_5$, corresponding to a ΔOD increase at about 1981 and 1943 cm^{-1}, together with the decomposition of $W(CO)_6$. The spectrum change, in which two new absorption bands at 1973 and 1952 cm^{-1} grow as $W(CO)_5$ decreases with two isosbestic points at about 1977 and 1964 cm^{-1}, suggests the formation of stoichiometric compounds. The IR absorption spectrum observed 3 μs after photolysis (Fig. 6b) is different from that of the fully relaxed $W(CO)_5$ shown by the broken line in the same figure. The $W(CO)_5Xe$ complex has an E mode C–O stretching at 1975 cm^{-1},[10] so the 1952-cm^{-1} band can be identified as the low frequency of the A_1 mode and the 1973-cm^{-1} band as the E mode of C_{4v} symmetry.

The Xe pressure effect on the transient absorption features after 355-nm laser photolysis of $W(CO)_6$ is

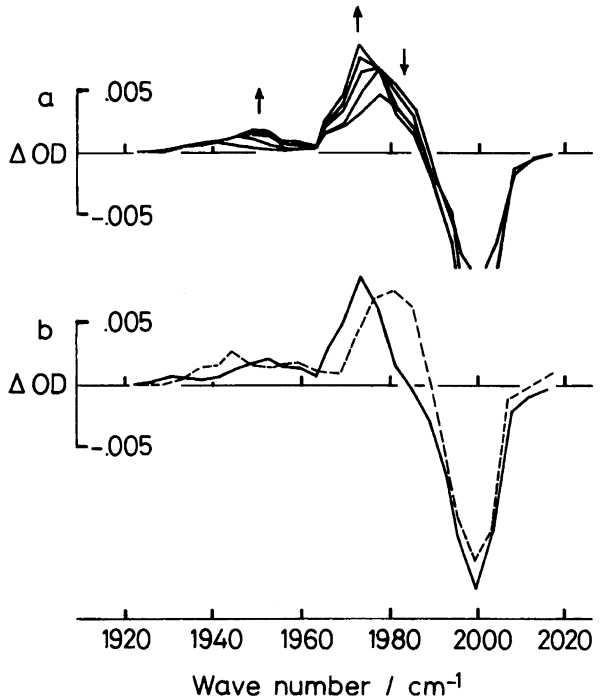

Fig. 6. TRIR spectra (a) after the 355-nm laser photolysis of a mixture of $W(CO)_6$ (ca. 10 mTorr) and Xe (6.0 Torr) at a total pressure of 10 Torr with balance Ar taken at 0.4-μs intervals over a 0.4- to 2.0-μs range. An arrow points upward indicates an increase of ΔOD and an arrow points downward indicates a decrease. Comparison of the infrared absorption spectrum of $W(CO)_5Xe$ complex (—) with that of fully relaxed $W(CO)_5$ (---), the former spectrum obtained 3 μs after 355-nm photolysis of this mixture and the latter spectrum obtained 1.5 μs after 355-nm photolysis of $W(CO)_6$ (ca. 10mTorr) at a total pressure of 6 Torr with balance Ar.

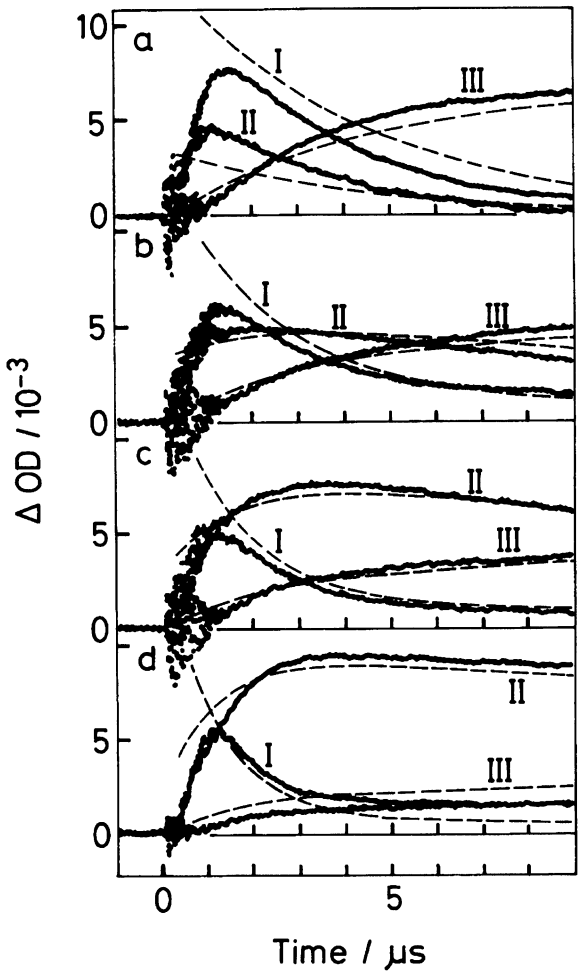

Fig. 7. Transient absorption at 1981 cm^{-1} (I, $W(CO)_5$), 1973 cm^{-1} (II, $W(CO)_5Xe$), and 1955 cm^{-1} (III, $W_2(CO)_{11}$) after the 355-nm laser photolysis of $W(CO)_6$ (ca. 10 mTorr) in the presence of (a) 0, (b) 2.0, (c), 4.0, and (d) 6.0 Torr Xe. Total pressure was 10 Torr with balance Ar. Dashed lines are simulation curves obtained with appropriate kinetic parameters. See text.

shown in Fig. 7. Curve I monitored at 1981 cm^{-1} shows the transient behavior of $W(CO)_5$. Curve II at 1973 cm^{-1} does the same for the $W(CO)_5Xe$ complex, which overlaps somewhat with the E band of $W(CO)_5$ centered at 1981 cm^{-1}. Curve III at 1955 cm^{-1} does the same for $W_2(CO)_{11}$, which overlaps slightly with the $W(CO)_5Xe$ complex. With increasing Xe pressure, the decay rate of curve I increases, the production rate of curve II increases, the amplitude of the absorbance at this wave number increases, the decay of this compound seems to slow, and the amplitude of absorbance at 1955 cm^{-1} (curve III) decreases. These results suggest that the addition of Xe suppresses the formation of the binuclear complex $W_2(CO)_{11}$. Wells and Weitz[10] have recently reported the observation of $M(CO)_5$(rare gas) complexes (M=Mo and W), and they proposed the equilibrium mechanism to be as follows:

$$M(CO)_5 + Xe \underset{k_{-4}}{\overset{k_4}{\rightleftharpoons}} M(CO)_5Xe \qquad (4)$$

Three transient features of Fig. 7 were simulated with reactions 1 and 4 (M=W). Some assumptions were introduced during the simulation for estimation of the rate constants of k_4 and k_{-4}. (1) The rate of reaction 1 ($=k_1$ [$W(CO)_6$]) is 2.3×10^5 s^{-1}; (2) the relative absorption coefficients among these three species, $W(CO)_5$, $W(CO)_5Xe$, and $W_2(CO)_{11}$, at each wave number are kept constant throughout the simulation; and (3) there is an overlap of the absorption bands of $W(CO)_5$ and $W(CO)_5Xe$ at 1973 cm^{-1}. Curve-fitting by eye was done for estimation of the rates of reactions 4 and −4. Better simulation curves are shown in Fig. 7 by the dashed lines, which are not corrected for the instrument time constants. The reproducibility of the transient behavior seems to be adequate although there is some discrepancy in the absorption intensity, perhaps caused by scattering in the concentration of $W(CO)_6$ or in the photolysis intensity from run to run. The coordination

rate (k_4[Xe], reaction 4) and the unimolecular decomposition rate (k_{-4}, reaction −4) are plotted against Xe pressure in Fig. 8. The second-order rate constant was inferred to be $(1.0\pm0.3)\times10^5$ $Torr^{-1}$ $s^{-1}$for k_4 and the first-order rate constant of $W(CO)_5Xe$ was inferred to be $(1.0\pm0.3)\times10^5$ s^{-1} for k_{-4}.

Discussion

Assignment of IR Absorption Bands in the Gas Phase. Our results for gas-phase tungsten pentacarbonyl complexes and earlier reported results for these species are listed in Table 1. Previous work on relevant group VI pentacarbonyl species is summarized in Table 2. There is some difficulty in comparison between IR absorption frequencies observed in the gas phase and in condensed phase mainly because of the solvent effect. For example, $W(CO)_6$ absorbs at 1997.6 cm^{-1} in the gas phase[22] but at 1988 cm^{-1} in an Ar matrix at 4 K and at about 1982 cm^{-1} in a CH_4 matrix at 20 K.[3b] Nevertheless, comparison may give qualitative evidence for the assignment of transient species in the gas phase. On the assumption that the solvent effect causes a red shift of about 20 cm^{-1} in C–O stretching bands, $W(CO)_5(NH_3)$ in the gas phase would be expected to have an E band at around 1950 cm^{-1} and an A_1 band at round 1935 cm^{-1} from the related amine complexes' frequencies in Table 2. These values coincide with our gas-phase results although the position of the A_1 band was not clear in our measurement. With the $W(CO)_5$(olefin) complex, the solvent effect with a red shift by about 15-cm^{-1} seems to be smaller than that with $W(CO)_5$(amine). An E band at around 1970 cm^{-1} and A_1 band at around 1985 cm^{-1} were estimated for $W(CO)_5(C_2H_4)$ in the gas phase; the estimates were consistent with our gas-phase results. The C–O stretching band at 1975 cm^{-1} of $Cr(CO)_5(C_2H_4)$, an overlap band of the E and A_1 modes, may also support the assignment of two bands at 1968 and 1985 cm^{-1} to $W(CO)_5(C_2H_4)$ because naked $Cr(CO)_5$ has similar IR absorption to naked $W(CO)_5$[23] and can be expected to have a similar interaction with a coordinating compound owing to the same electron configuration, d^6, at the metal center. The IR spectrum observed after the 355-nm photolysis of $W(CO)_6$ in the presence of Xe is consistent with that reported for $W(CO)_5Xe$ by Wells and Weitz,[10] and with the results obtained in the condensed phase shown in Table 2, if the solvent effect is allowed for as we suggest.

As the solvent effect involves many factors such as the solvent, ligand, and phase, comparison with rigid-phase spectroscopy would make possible only an indirect assignment of the gas-phase spectrum. Kinetic analysis and interaction considerations may justify the assignment of transient IR absorption bands observed after 355-nm laser photolysis of $W(CO)_6$ in the presence of L (L=NH_3, C_2H_4, or Xe) to the simple coordination compound $W(CO)_5L$.

Interaction of NH_3 and C_2H_4 with $W(CO)_5$. Figure 9 shows a molecular orbital diagram for the interaction of a σ-bond of NH_3 and π- and π*-bonds of C_2H_4 with $W(CO)_5$, constructed based on MO calculations[24,25] and on the picture proposed by Andrea's group.[26] When the $W(CO)_5$ is bonded to a strong σ-donor ligand such as NH_3, the frequency of the E mode (equatorial C–O stretching) is lowered (1980→1950 cm^{-1}) but that of the A_1 mode (axial C–O stretching) shifts little (1942→ca. 1942 cm^{-1}). This dif-

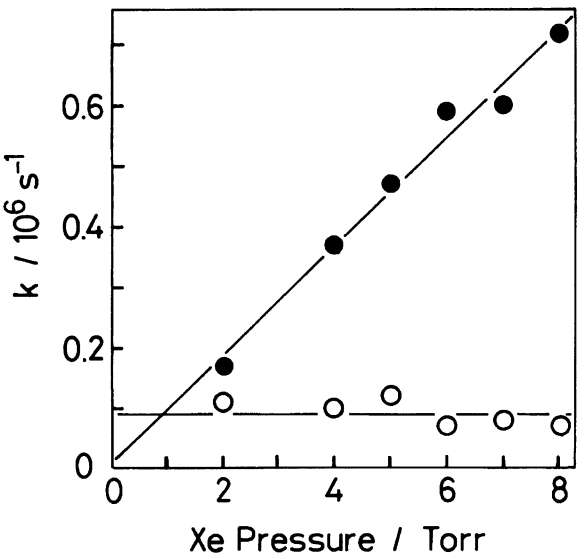

Fig. 8. Xe pressure dependence of the association rates (●; reaction 4, k_4[Xe]) and the unimolecular decomposition rates of $W(CO)_5Xe$ (○; reaction 5, k_5) after 355-nm laser photolysis of mixtures of $W(CO)_6$ (ca. 10 mTorr) and Xe at a total pressure of 10 Torr with balance Ar. Both rates were derived from the simulation of the transient absorptions at 1981 cm^{-1} ($W(CO)_5$), 1973 cm^{-1} (overlap of $W(CO)_5$ and $W(CO)_5Xe$), and 1955 cm^{-1} ($W_2(CO)_{11}$) in Fig. 7.

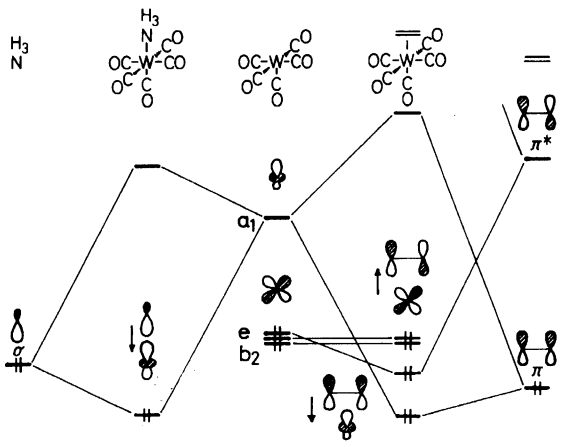

Fig. 9. Interaction of the coordination of NH_3 as a typical σ-donor and C_2H_4 as a typical π-acceptor onto $W(CO)_5$. The arrow indicates the electron flow.

Table 1. Infrared Frequencies (cm^{-1}) in the C–O Stretching Region of $W(CO)_5L$ Complexes ($L=NH_3$, C_2H_4, and Xe)

Complex	ν(CO)/cm^{-1}		Ref.[a]
	E	A_1	
$W(CO)_5(NH_3)$	1950	(1942)	This work, at r.t., in gas phase.
$W(CO)_5(C_2H_4)$	1953	1973	2a, at r.t., in hexane sol.
	1955.5	1974	11b, at r.t., in pentane sol.
	1947	1968	11a, at 77 K, in MCH glass.
	1968	1985	This work, at r.t., in gas phase.
$W(CO)_5Xe$	1975		10, at r.t., in gas phase.
	1973	1952	This work, at r.t., in gas phase.

a) r.t., room temperature.

Table 2. Representative Infrared Frequencies (cm^{-1}) in the C–O Stretching Region Associated with This Measurement

Complex	ν(CO)/cm^{-1}		Ref.[a]
	E	A_1	
$W(CO)_5(Et_2NH)$	1930	1913	32, at r.t., in 2,2,4-trimethylpentane sol.
$Cr(CO)_5(NHC_5H_{10})$	1933.4	1916.3	33, at r.t., in heptane sol.
$Cr(CO)_5(C_2H_4)$	1975		34, at r.t., in gas phase.
	1960.4	1967.4	11b, at 253 K, in pentene sol.
$Cr(CO)_5Xe$	1964.9	1939.1	3b, at 20 K, in Ar-2%Xe matrix.
$W(CO)_5Ar$	1963.3	1932.2	3a, at 20 K, in Ar matrix.
$W(CO)_5$	1980	1942	19, at r.t., gas phase.
$Cr(CO)_5$	1980	1948	23, at r.t., gas phase.

a) r.t., room temperature.

ference can be interpreted as the interaction of an overlap of the σ-orbital of NH_3 with the a_1-orbital d(z^2) of W, which is mixed with π*-bonds of the equatorial COs with a_1 symmetry as follows (Chart 1). For $Mn(CO)_5$, the a_1-orbital has the calculated composition of 21% d(z^2), 18% p, 1% apical (approximately axial) CO, and 56% all basal (approximately equatorial) COs.[24] Both π- and π*-bonds participate in mixing of a_1 orbitals, but the electron flows more easily into a π*-orbital than a π-orbital because π*-orbital concentrated at carbon and, of course, the electron density of the π*- orbital is lower than that of the π-orbital. This interaction results in a weakening of equatorial C–O bonds by the net electron flow from the σ-orbital of NH_3 to π*-orbitals of COs. This mechanism cannot be distinguished from direct overlap between the σ-bonding orbital of NH_3 with the π*-orbitals of the equatorial COs.[27] On the other hand, the coordination of a π-acceptor such as C_2H_4 decrease the E-mode frequency (1980→1968 cm^{-1}) and increases the A_1-mode frequency (1942→1985 cm^{-1}). This finding suggests that the main interaction is in an overlap of π*-orbitals of C_2H_4 and one component of the e set mixed with π*-orbitals of axial CO as follows (Chart 2). Then the bond strength of C–O increases owing to an electron flow from the π*-orbital of axial CO to the π*-orbital of C_2H_4. This phenomenon is the essence of the Dewar-Chatt-Duncanson model for metal-olefin bonding.[25,28] It also is a rough picture of the weakening of double bonding by coordinated olefin, resulting in olefin isomerization or in olefin hydrogenation in homogeneous catalysis involving a transition metal center. In olefin hydrogenation, the weakening of the bonding of H–H owing to the π-acceptor-like character of H_2 coordination at the metal center would also have some effect.[29] The decrease in the frequency of the E mode suggests a slight overlap between the π-bond of C_2H_4 and the a_1-orbital of $W(CO)_5$.

Interaction of Xe with $W(CO)_5$. The binding energy of Xe coordination at the tungsten center can be evaluated by statistical mechanics from the equilibrium constant, K_p, measured at a single temperature. On the

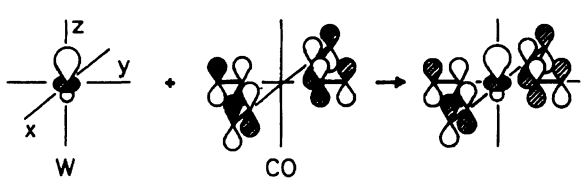

Chart 1.

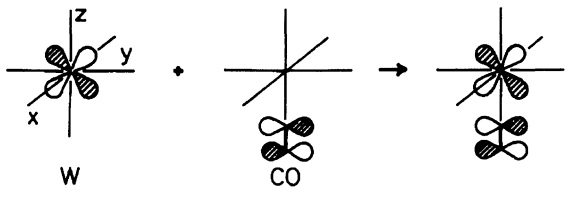

Chart 2.

assumption that the vibrational frequencies of $W(CO)_5$ are not changed in the complex, then K_p, in terms of the binding energy, ΔE_0, simplifies to:

$$K_p = \frac{(z_r z_t \Pi z_i)_{W(CO)_5Xe}}{(z_r z_t)_{W(CO)_5}(z_t)_{Xe}} \exp(-\Delta E_0/RT)$$

where z_t and z_r are translational and rotational partition functions and z_i ($i=1$, 2, and 3) are partition functions associated with the three extra internal degrees of freedom of the complex. The following geometrical parameters were used in the estimation of the internal moment of $W(CO)_5$: r(C=O), 115 pm; r(W–C), 206 pm; Θ_a (C–W–C), 90° ; Θ_b (C–W–C), 180°.[30] The bond length of W and Xe was assumed to be 300 pm, which is an estimated length for Mo–Kr in the $Mo(CO)_5Kr$ complex.[31] z_i were calculated assuming there were one vibration (W-Xe stretch) at 200 cm^{-1} and two vibrations (W-Xe bend) at 100 cm^{-1}. These values of K_p (=1.0 $Torr^{-1}$) give $\Delta E_0=8.3$ kcal mol^{-1}. If a rigid complex is assumed, i. e., $z_i=1$, then $\Delta E_0=9.8$ kcal mol^{-1}, if a loose complex with three vibrations at 50 cm^{-1} is assumed, then $\Delta E_0=7.0$ kcal mol^{-1}. Wells and Weitz reported that the activation energy of reaction -4 was 7.4 ± 1.0 kcal mol^{-1} from their temperature study;[10] this value is in fair agreement with the range of third-law values. The agreement suggests that $W(CO)_5Xe$ favors a loose complex.

The interaction of $W(CO)_5$-Xe may be explained by the weak σ-donation from Xe to the W center, as observed for $W(CO)_5$(alkane).[8] The red shift in the E band (1981→1973 cm^{-1}) is caused by net electron flow from Xe to the a_1 orbital involving π^*-orbitals of equatorial COs (Fig. 10). The small blue shift in the A_1 band (1943→1952 cm^{-1}) may be due to the decrease in π-back-donation to axial CO caused by a slight decrease in the overlap between d(yz or zx) and π^*-orbital of axial CO, because the a_1-orbital is strongly metal-axial ligand-antibonding,[24] and because an inflow of electrons in the a_1-orbital would weaken W–CO bonding.

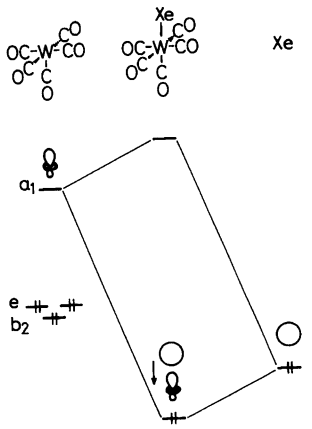

Fig. 10. Interaction of the coordination of Xe onto $W(CO)_5$. The arrow indicates the electron flow.

We thank Dr. D. M. Rayner and Dr. P. A. Hackett for valuable discussion in the early stage of this work. We also thank Professors Y. Nosaka, and M. Koshi, and Dr. T. Munakata for helpful suggestions for the construction of the experimental setup. This work was supported by a Grant-in-Aid for Scientific Research No. 02640342 from the Ministry of Education, Science and Culture.

References

1) I. W. Stolz, G. R. Dobson, and R. K. Sheline, *J. Am. Chem. Soc.*, **84**, 3589 (1962).

2) a) I. W. Stolz, G. R. Dobson, and R. K. Sheline, *Inorg. Chem.*, **2**, 1264 (1963); b) M. A. Graham, R. N. Perutz, M. Poliakoff, and J. J. Turner, *J. Organomet. Chem.*, **34**, C34 (1972); c) J. D. Black and P. S. Braterman, *J. Am. Chem. Soc.*, **97**, 2908 (1975); d) D. R. Tyler and D. P. Perylak, *J. Organomet. Chem.*, **212**, 389 (1981); e) R. H. Hooker and A. J. Rest, *J. Organomet. Chem.*, **249**, 137 (1983).

3) a) M. A. Graham, M. Poliakoff, and J. J. Turner, *J. Chem. Soc. A*, **1971**, 2939; b) R. N. Perutz and J. J. Turner, *J. Am. Chem. Soc.*, **97**, 4791 (1975); c) J. K. Burdett, M. A. Graham, R. N. Perutz, M. Poliakoff, A. J. Rest, J. J. Turner, and R. F. Turner, *J. Am. Chem. Soc.*, **97**, 4805 (1975).

4) A. G. Joly and K. A. Nelson, *J. Phys. Chem.*, **93**, 2876 (1989).

5) a) J. D. Simon and K. S. Peters, *Chem. Phys. Lett.*, **98**, 53 (1983); b) J. D. Simon and X. Xie, *J. Phys. Chem.*, **91**, 5538 (1987).

6) a) J. E. Huheey, "Inorganic Chemistry," Harper & Row, (1983), p. 433; b) K. Nakamoto, "Infrared and Raman Spectra," Wiley-Interscience, (1986), p. 291.

7) E. Weitz, *J. Phys. Chem.*, **91**, 3945 (1987), and references cited therein.

8) a) Y. Ishikawa, C. E. Brown, P. A. Hackett, and D. M. Rayner, *Chem. Phys. Lett.*, **150**, 506 (1988); b) C. E. Brown, Y. Ishikawa, P. A. Hackett, and D. M. Rayner, *J. Am. Chem. Soc.*, **112**, 2530 (1990).

9) P. L. Bogdan, J. R. Wells, and E. Weitz, *J. Am. Chem. Soc.*, **113**, 1294 (1991).

10) J. R. Wells and E. Weitz, *J. Am. Chem. Soc.*, **114**, 2783 (1992).

11) a) K. R. Pope and M. S. Wrighton, *Inorg. Chem.*, **24**, 2792 (1985); b) F. Grevels, J. Jacke, and S. Ozkar, *J. Am. Chem. Soc.*, **109**, 7536 (1987); c) M. Wrighton, *Inorg. Chem.*, **13**, 905 (1974).

12) I. Wender, "Organic Syntheses via Metal Carbonyls," Interscience Publishers, New York (1968), Vol. 1.

13) M. Jyo-o, K. Omiya, Y. Ishikawa, and S. Arai, *Chem. Lett.*, **1992**, 2205.

14) B. I. Sonobe, T. R. Fletcher, and R. N. Rosenfeld, *J. Am. Chem. Soc.*, **106**, 4352 (1984).

15) A. J. Dixon, M. A. Healy, P. M. Hodges, B. D. Moore, M. Poliakoff, M. B. Simpson, J. J. Turner, and M. A. West, *J. Chem. Soc., Faraday Trans.*, **82**, 2083 (1986).

16) A. J. Ouderkirk, P. Wermer, N. L. Schultz, and E. Weitz, *J. Am. Chem. Soc.*, **105**, 3354 (1983).

17) a) D. M. Rayner, A. S. Nazran, M. Drouin, and P. A. Hackett, *J. Phys. Chem.*, **90**, 2882 (1986); b) Y. Ishikawa, P. A. Hackett, and D. M. Rayner, *J. Am. Chem. Soc.*, **109**,

6644 (1987).
18) a) N. Djeu, *Appl. Phys. Lett.*, **23**, 309 (1973); b) J. Puerta, W. Herrmann, G. Bourauel, and W. Urban, *Appl. Phys.*, **19**, 439 (1979).
19) Y. Ishikawa, P. A. Hackett, and D. M. Rayner, *J. Phys. Chem.*, **92**, 3863 (1988).
20) P. J. Hay, *J. Am. Chem. Soc.*, **100**, 2411 (1978).
21) L. E. Orgel, *Inorg. Chem.*, **1**, 25 (1962).
22) L. H. Jones, R. S. McDowell, and M. Goldblatt, *Inorg. Chem.*, **8**, 2349 (1969).
23) T. A. Seder, S. P. Church, and E. Weitz, *J. Am. Chem. Soc.*, **108**, 4721 (1986).
24) M. Elian and R. Hoffmann, *Inorg. Chem.*, **14**, 1058 (1975).
25) T. A. Albright, J. K. Burdett, and M. H. Whangbo, "Orbital Interactions in Chemistry," Wiley-Interscience, New York (1985).
26) R. R. Andrea, M. A. Vuurman, D. J. Stufkens, and Ad Oskam, *Recl. Trav. Chim. Pays-Bas*, **105**, 372 (1986).
27) R. F. Fenske and R. L. DeKock, *Inorg. Chem.*, **9**, 1053 (1970).
28) M. J. S. Dewar and G. P. Ford, *J. Am. Chem. Soc.*, **101**, 783 (1979).
29) a) Y. Ishikawa, R. A. Weersink, P. A. Hackett, and D. M. Rayner, *Chem. Phys. Lett.*, **142**, 271 (1987); b) Y. Ishikawa, P. A. Hackett, and D. M. Rayner, *J. Phys. Chem.*, **93**, 652 (1989).
30) C. M. Luckehart, "Fundamental Transition Metal Organometallic Chemistry," Brook-Cole, Monterey (1985).
31) A. Rossi, E. Kochanski, and A. Veillard, *Chem. Phys. Lett.*, **66**, 13 (1979).
32) R. A. Brown and D. R. Dobson, *Inorg. Chim. Acta*, **6**, 65 (1972).
33) D. J. Darensbourg and M. A. Murphy, *Inorg. Chem.*, **17**, 884 (1978).
34) B. H. Weiller and E. R. Grant, *J. Am. Chem. Soc.*, **109**, 1252 (1987).